Check for updates

GEP- and MLR-based equations for stable channel analysis

Mohd Afiq Harun [a,*], Aminuddin Ab. Ghani [a], Reza Mohammadpour [b] and Ngai Weng Chan [c]

[a] River Engineering and Urban Drainage Research Centre (REDAC), Universiti Sains Malaysia, Engineering Campus, 14300 Nibong Tebal, Penang, Malaysia
[b] Department of Civil Engineering, Estahban Branch, Islamic Azad University, Estaban, Iran
[c] School of Humanities, Universiti Sains Malaysia, 11800 Penang, Malaysia
*Corresponding author. E-mail: mohdafiq.harun@yahoo.com

MAH, 0000-0002-9210-3466; AAG, 0000-0002-8912-9569; RM, 0000-0002-7940-5101; NWC, 0000-0003-3257-3922

ABSTRACT

For decades, research on stable channel hydraulic geometry was based on the following parameters: river discharge, dimensionless discharge, the median size of bed material and the slope. Although significant research has been conducted in this area, including applied machine learning to increase the geometry model prediction accuracy, there has been no remarkable improvement as the variables used to describe the geometry relationship remain the same. The novelty of this study is demonstrated by the parameters used in the stable channel geometry equations that outperform the existing equation's accuracy. In this research, sediment transport parameters are introduced and analysed by applying the multiple linear regression (MLR) and gene expression programming (GEP) methods. The new equation of the width, depth and bed slope can give much-improved results in efficiency and lower errors. Furthermore, a new parameter B/y is introduced in this study to solve the restriction issue, either in width or depth prediction. The results from MLR and GEP show that in addition to the existing hydraulic geometry parameter, the B/y parameter is also able to give high accuracy results for width and depth predictions. Both calibration and validation for the B/y parameter yield high R^2 and NSE values with low mean squared errors and mean absolute errors.

Key words: GEP, MLR, stable channel

HIGHLIGHTS

- Review of the performance of the existing stable channel geometry equations.
- Introduction of the sediment transport parameters in the development of the stable channel geometry equations.
- Application of multiple linear regression and gene expression programming methods.
- New parameter B/y is introduced to predict the width and depth of a stable channel.
- Newly developed equations outperformed the existing conventional equation.

GRAPHICAL ABSTRACT
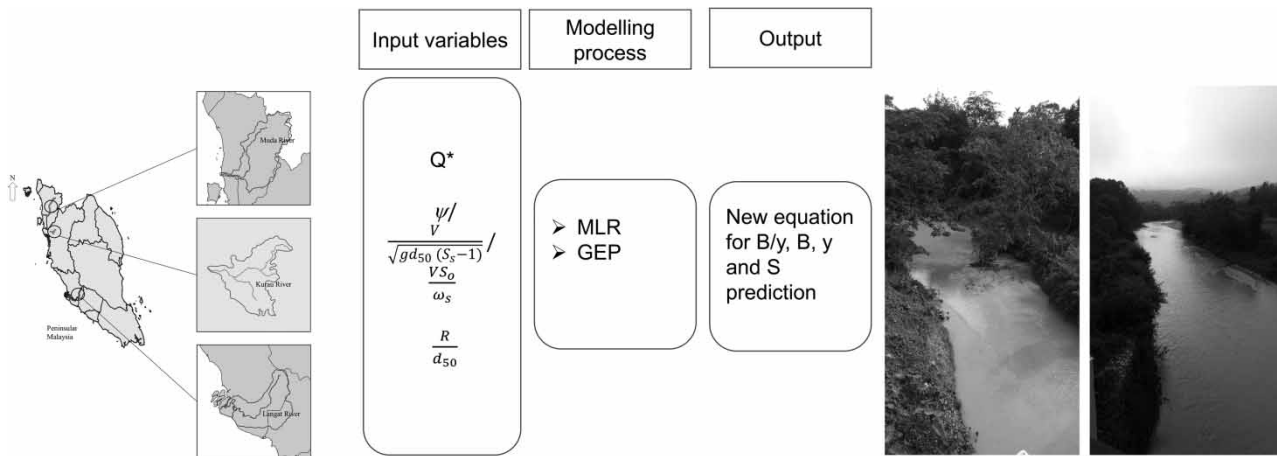
INTRODUCTION

A stable channel can be described by a balance of erosion and sedimentation processes that produce average dimensions, which do not change significantly over the years (Bonakdari *et al.* 2020). It is essential to estimate the dimension correctly to minimise the erosion and sedimentation effect (Garcia 2008). The prediction of a stable channel depends on various parameters and is described by the characteristics of the top width of the channel, the mean depth of the flow and the longitudinal slope (Bonakdari *et al.* 2020). For decades, researchers tried to correlate channel geometry to the geomorphological variables. According to Chang (1988) and Garcia (2008), a stable channel was determined by empirical and analytical methods. Blench (1957), Lacey (1930), Lindley (1919), Kennedy (1895) and Simons & Albertson (1960) investigated the regime concept by examining the channel stability parameters by using statistical methods. Leopold & Maddock (1953) introduced the concept of power function theory, and this theory has been the method of choice for many researchers. Channel geometry is described by the corresponding water and sediment discharge. The researchers divided this method into two categories, namely, downstream hydraulic geometry and at-a-station hydraulic geometry. By applying the hydraulic geometry method, Julien & Wargadalam (1995) extended this concept by introducing the relationship between the channel geometry and the full bank discharge (Q), the median size of bed material (d_{50}), the channel bed slope (S) and the Shields parameter (τ^*). The width, mean depth and velocity depend on Q, d_{50} and S, while the channel slope is dependent on Q, d_{50} and τ^*. Lee & Julien (2007) extended this research by using statistical analysis, and the new equations were found to be more accurate than the previous equations as a broader range of data was used in the study. Afzalimehr *et al.* (2010) investigated the relationship of channel geometry by using the at-a-station method and discovered that the median size of bed material and the Shields parameter did not contribute much to the width and depth. Other researchers, such as Kaless *et al.* (2014), Parker (1978), Parker (1979) and Pitlick & Cress (2002), use dimensionless width (B^*), depth (y^*) and dimensionless discharge (Q^*) to describe the relationship of stable channel geometry. The variable B^* is defined by B/d_{50} and y^* is presented by y/d_{50}, while Q^* is defined by $Q/\left(\sqrt{Rgd_{50}}\ d_{50}^2\right)$, where R is the submerged specific gravity of the sediment, assumed 1.65, and g is the standard gravity acceleration. The previous equations for stable channel design are shown in Table 1.

In the analytical approach, the design of the stable channel is controlled by the dominant process within the channel, such as flow resistance or sediment transport (Garcia 2008). The rational method proposed by Chang (1988), for instance, adopted three equations that are unique to the three dependent variables: width, depth and slope. Other methods derived from the analytical approach include those of Abou-Seida & Saleh (1987), Copeland (1994) and Yalin & da Silva (2000). The analytical method is very flexible, since the program enables the user to predict the stable channel geometry with the restriction in the depth or width of the river (Jang *et al.* 2016; Harun *et al.* 2020). The drawback of this method is its dependence on the accuracy of the sediment transport equation. Singh (2003) and Deshpande & Kumar (2012), however, use the concept of maximum entropy/minimum energy principle to examine the regime relationship for hydraulic geometry prediction. Gholami *et al.* (2018, 2019a, 2019b) also applied these concepts in predicting bank profile shape, and the results show that the method is capable of predicting geometry with better results. Bonakdari *et al.* (2020) asserted that rational approaches

Table 1 | Existing equations for the design of stable channel

Researchers	Width (B)	Depth (y)	Slope (S)
Simons & Alberstone (1960)	$2.85Q^{0.5}$	$2.85Q^{0.36}$	$0.0062Q^{-0.24}$
Hey & Thorne (1986)	$3.67Q^{0.45}$	$0.22Q^{0.37}d_{50}^{-0.11}$	$0.096Q^{-0.31}d_{50}^{0.71}$
Julien & Wargadalam (1995)	$1.33Q^{0.44}d_5^{-0.11}S^{-0.22}$	$0.2Q^{0.33}d_{50}^{0.17}S^{-0.17}$	$12.4Q^{0.4}d_s\tau^{*1.2}$
Pitlick & Cress (2002)	$39.3Q^{*0.32}$	$0.07Q^{*0.53}$	$0.78Q^{*-0.5}$
Lee & Julien (2007)	$3.004Q^{0.426}d_{50}^{-0.002}S^{-0.153}$	$0.201Q^{0.336}d_{50}^{-0.025}S^{-0.060}$	$4.981Q^{0.346}d_{50}^{0.955}\tau^{*0.966}$
Afzalimehr et al. (2010)	$5.876Q^{0.743}$	$0.226Q^{0.345}$	$1.565d_{50}^{0.821}\tau^{*0.851}$
Abdelhaleem et al. (2016)	–	$0.717Q^{0.319}d_{50}^{-0.08}$	$12.5Q^{-0.156}d_{50}^{0.42}$
Haron et al. (2019)	$12.3Q^{0.2}$	$0.9Q^{0.5}$	–

seem to be complicated and require a deep understanding of fluid flow, which is often time-consuming. Bonakdari *et al.* (2020) suggested including different key geomorphological variables to increase the prediction accuracy.

Currently, the use of machine learning in water resources engineering has been the method of choice for many researchers (Muhammad *et al.* 2018; Kargar *et al.* 2019; Montes *et al.* 2020; Roushangar & Shahnazi 2020; Sharafati *et al.* 2020). This method was extensively investigated by Gholami *et al.* (2019a, 2019b) and Shaghaghi *et al.* (2018) for use in a stable channel. Machine learning can be applied by using various methods such as artificial neural networks, adaptive network-based fuzzy inference systems, support vector machines, gene expression programming (GEP) and evolutionary polynomial regression (EPR) (Giustolisi & Savic 2009; Ebtehaj *et al.* 2019; Khosravi & Javan 2019; Roushangar & Ghasempour 2019; Yahaya 2019; Asheghi *et al.* 2020; Najafzadeh & Oliveto 2020). The research done by Bonakdari *et al.* (2020) showed that GEP and EPR had improved the accuracy of the model prediction; however, the improvement is not remarkable compared to the original equation.

These earlier findings suggest that a new equation should be developed to increase the accuracy of stable channel prediction. To date, many researchers have focused on parameters Q, d_{50} S_o and Q^* to determine stable channel geometry. This paper will focus on introducing a new equation for stable channel geometry by adopting sediment transport parameters that resemble the hydraulic characteristic of the river. The width/depth (B/y) parameter will be introduced to the equation for predicting stable channel geometry to solve the problem when there is a restriction in width or depth, as discussed earlier in the analytical approach. The proposed equation will be further enhanced by using the machine learning method to increase the model prediction accuracy.

MATERIALS AND METHODS

Multiple linear regression

This study uses ordinary multiple regression in linearised form after log transforming all the variables included in the equation. Since all the possible test cases are described in one power law equation, the fitting of all regressions can be determined using statistical analysis software, Statistical Product and Service Solutions (SPSS). The dependent variable used for this equation is B^*, y^*, S_o and B/y.

Gene expression programming

GEP has been developed as an extension to genetic programming (Koza 1994). This program involved several search techniques, such as decision trees and logical expression, that help to evolve computer programs. GEP is encoded in linear chromosomes that can be represented by an expression tree (ET). With the aim to analyse particular data through genetic modification, the population of an ET will adapt and discover the traits of the data. The decision tree and logical expression have to be initially carefully determined to ensure the program yields the best results (Ferreira 2001b). The chromosome of each individual is randomly selected and evaluated by the fitness function and selected by the genetic operator to reproduce with modification (mutation). The same process occurs in the new individual for whom the trends are repeated until the required accuracy is obtained (Ferreira 2001a, 2001b). Figure 1 summarises the steps taken to execute the GEP. The data are first randomised before continuing to the next step. Approximately, 80% of the data are used for training and the
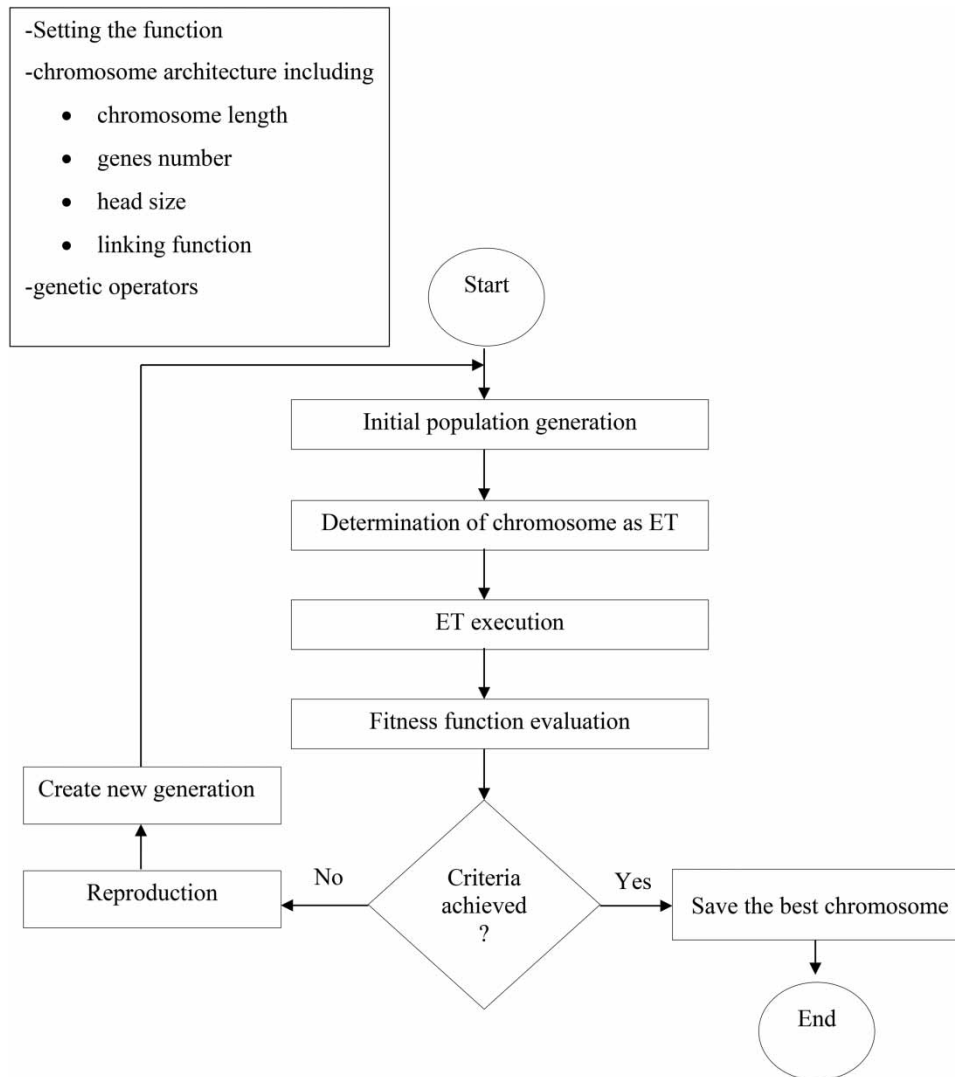
Figure 1 | GEP flow chart for the stable channel geometry prediction.

remaining data for testing purposes. The setting of the function and chromosome architecture includes chromosome length, gene number, head size, linking function and genetic operators. The root-mean-square error (RMSE) was used as a fitness function to fit the curve to the target value. The stopping criteria were set at 25,000 generations for all the runs of the various models. The summarised parameters used in the GEP model are shown in Table 2.

Study area

The river data used in this study were obtained from the Malaysian Department of Irrigation and Drainage. Three rivers were chosen for the study to represent different hydraulic characteristics of a large river (Muda River), a medium river (Langat River) and a small river (Kurau River). The locations of these rivers are shown in Figure 2.

Muda River Basin

The Muda River originates in the highland areas of Kedah, a northern state of Malaysia, which borders Thailand. It is the largest river in Kedah and is important in supplying water to the three states of Kedah, Perlis and Pulau Pinang (Sim et al. 2015). The Muda River Basin covers a drainage area of 4,210 km². In terms of length, the Muda River is approximately 180 km long, with a slope of 1/2,300 (or 0.00043). The channel width of the Muda River is typically around 10 m upstream, 100 m in midstream and widest at its estuary, averaging 300 m (DID 2009). In terms of depth, bathymetric surveys show that

Table 2 | Operators and values of parameters used in the GEP model

Parameter type	Parameter	Value
General setting	Generation number	25,000
	Function set	$+, -, \times, /, \sqrt{}$, power
Architecture of chromosome	Chromosome length	80
	Gene numbers	3
	Head size	8
	Linking function	Addition $(+)$
Genetic operators	Mutation rate	0.1
	Inversion	0.1
	Transposition	0.1
	One-point recombination	0.1
	Two-point recombination	0.1
	Gene recombination rate	0.1
	Gene transportation rate	0.1

the shallowest point in the river is located 2.5 km upstream from the river mouth, resulting in difficulty for navigation during low tides (Julien *et al.* 2010).

Langat River Basin

The Langat River forms one of the four major river systems in the state of Selangor. The Langat River is a medium-sized river, approximately 180 km long with an average annual flow of 35 m^3/s and a mean annual flood of 300 m^3/s. The Langat River system flows from the north-eastern state of Selangor to Negeri Sembilan and the Federal Territory of Putrajaya, finally emptying into the Straits of Malacca. The Langat River Basin has a total catchment area of 2,396 km^2 (DID 2009).

Kurau River Basin

The Kurau River Basin is a typically small river basin, draining an area of approximately 682 km^2. In terms of elevation, elevations at the river headwaters are moderately high, being 900–1,200 m. In terms of slopes, the upper 6.5 km of the river averaged 12.5%, while those lower down the valleys are significantly lower, in the order of 0.25–5%. The average velocity of the Kurau River ranges from 0.45 to 0.636 m/s with the highest sediment load being 0.878 kg/s (Saleh *et al.* 2018). A reservoir was constructed at the middle section of the river, approximately 65 km upstream. Two major systems, the Kurau River system and the Merah River system, are upstream of this reservoir, and both rivers drain into the reservoir (DID 2009).

Field data collection

River surveys, flow measurements and field data collection were conducted based on the *Guidelines for Field Data Collection and Analysis of River Sediment* by Ab. Ghani *et al.* (2003). The data collection includes flow discharge, bed and bank material, suspended load, bedload and water surface slope. In addition, bed elevation, water surface and thalweg measurements were also conducted at selected cross-sections. The range of the data for this study is shown in Table 3.

Development of new equations for stable channel geometry

The new equations were formulated by using dimensionless hydraulic geometry relations as proposed by Kaless *et al.* (2014), Parker (1978), Parker (1979) and Pitlick & Cress (2002). Along with the dimensionless stable geometry equation in terms of B^*, y^* and S, a new dimensionless B/y equation was introduced to solve the restriction issue in either width or depth prediction. The equation also uses dimensionless full bank discharge Q^* as one of the parameters in the development of the equation.

Researchers have divided the significant parameters that contribute to sediment transport into four-parameter classes, namely, mobility, transport, sediment and flow resistance (Ebtehaj & Bonakdari 2016; Harun *et al.* 2020). This concept has been widely used by researchers to define the sediment transport in the river (Sinnakaudan *et al.* 2006; Harun *et al.* 2020), in closed channels or in pipes (Ebtehaj *et al.* 2019; Danandeh Mehr & Safari 2020). These parameters were also
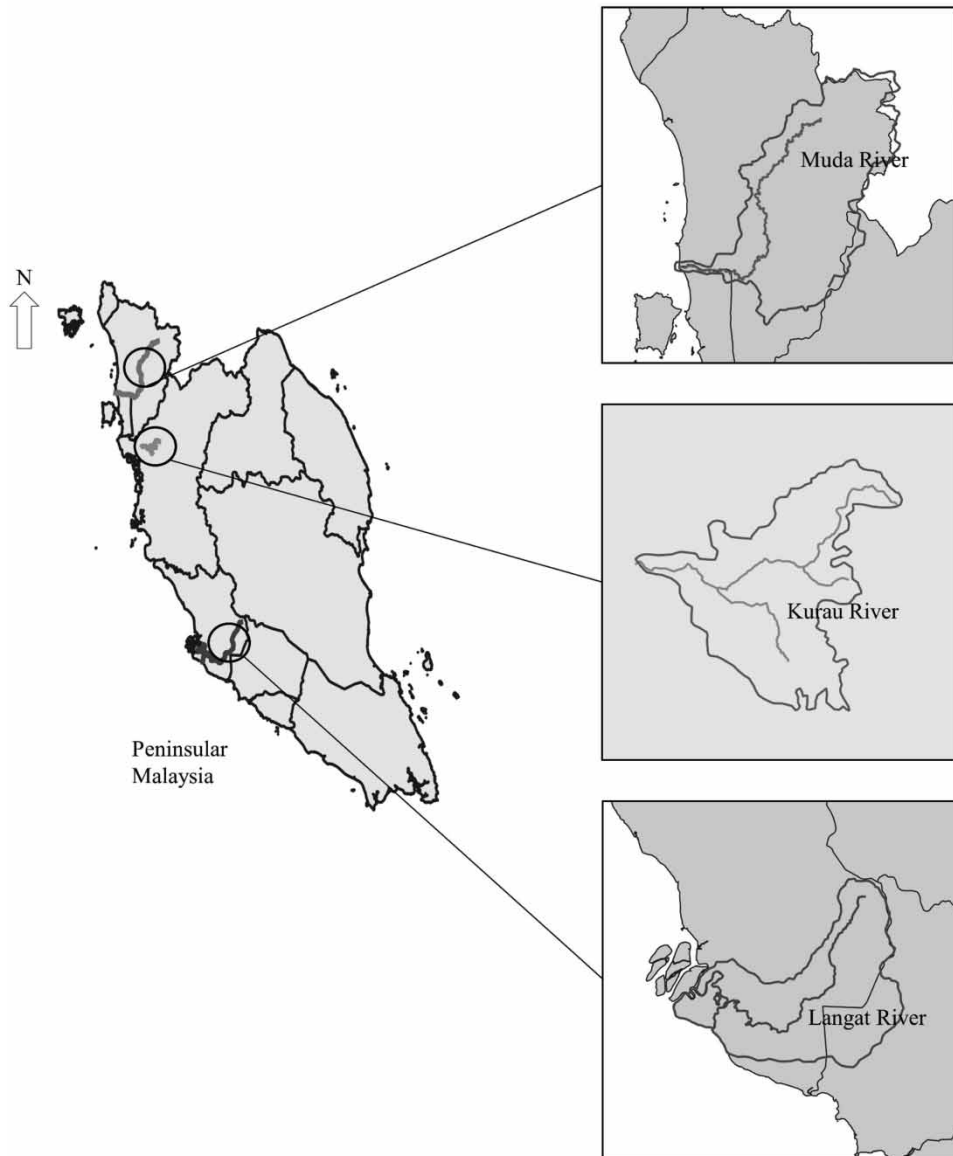
Figure 2 | Location of study areas.

found to be prevalent in the application of sewer sedimentation analysis (Ebtehaj & Bonakdari 2017; Kargar *et al.* 2019). The details of the parameters are shown in Table 4.

These parameters were combined to get the best relationship with regard to the dimensionless hydraulic geometry relations to width, depth, slope and width/depth. The parameters governing the stable channel geometry are presented in a dimensionless form, where ψ is the flow parameter, R is the hydraulic radius, U^* is the shear velocity, S_o is the bed slope, S_s is the specific gravity of the sediment, ω_s is the fall velocity of the bed material, V is the cross-sectional velocity, g is the acceleration due to gravity, A is the area of cross-section, v is the kinematic viscosity of water, ϕ is the transport parameter, D_{gr} is the dimensionless grain size and λ_s is the friction factor.

Goodness of fit of model performance

The equations were evaluated by using several indices, namely, R^2, Nash–Sutcliffe efficiency coefficient (NSE), mean squared error (MSE), mean absolute error (MAE) and discrepancy ratio (DR). Different statistical indexes used are presented in Equations (1)–(5), where O_i and P_i are the observed and predicted values, while $\bar{O}_i$ and $\bar{P}_i$ are the mean observed and

Table 3 | Range of river data for the current study

Variable/parameter	Current study (Muda River, Langat River and Kurau River)
Number of data sets	234
Discharge, Q (m³/s)	0.478–343.710
Average velocity, V (m/s)	0.140–1.450
River width, B	6.30–90.00
Flow mean depth, y	0.244–3.093
Cross-sectional area (m²)	1.430–278.34
Hydraulic radius, R (m)	0.174–3.900
Bed slope, S_o	0.00008–0.0009
Median diameter of the bedload, d_{50} (mm)	0.29–3.00
Total load (kg/s)	0.0178–99.40

Table 4 | Significant dimensionless parameters controlling sediment transport

Parameter class	Dimensionless groups
Mobility	$\psi = \dfrac{(S_s - 1)d_{50}}{RS_o},\ \dfrac{V}{\sqrt{gd_{50}\,(S_s - 1)}},\ \dfrac{U^*}{V},\ \dfrac{VS_o}{\omega_s}$
Transport	$C_v,\ \phi = \dfrac{C_v VR}{\sqrt{g\,(S_s - 1)d_{50}^3}}$
Sediment	$D_{gr} = d_{50}\left(\dfrac{g\,(S_s - 1)}{v^2}\right)^{1/3},\ \dfrac{U^*}{\omega_s},\ \dfrac{\omega_s d_{50}}{v},\ \dfrac{\omega_s}{U^*}$
Flow resistance	$R/d_{50},\ \lambda_s = \dfrac{8gRS}{V^2}$

Sources: Ariffin (2004), Harun et al. (2020) and Sinnakaudan et al. (2006).

predicted values. R^2 represents the correlation between measured and modelled values, MSE is the calculated mean error in the form of data units squared and MAE represents the absolute error between the measured and modelled values. In large events, MAE helps to reduce bias (Bennett et al. 2013). The NSE is used to describe how much the modelling error is to the variance of the observed data. One is the perfect value for the NSE; an NSE less than 0 indicates that the predicted model is unreliable and an NSE value closer to 1 represents high accuracy between the observed and the predicted model (Bonakdari et al. 2020; Danandeh Mehr & Safari 2020). The discrepancy ratio is the comparison between the computed and measured stable channel geometry. The acceptable range of DR values is between 0.5 and 2.0 (Julien & Wargadalam 1995; Lee & Julien 2007; Hadadin 2017), 0.5 and 1.5 (Afzalimehr et al. 2010), 0.8 and 1.2 (Abdelhaleem et al. 2016; Shaghaghi et al. 2018; Gholami et al. 2019b), 0.9 and 1.1 (Gholami et al. 2017) and the perfect correlation of computed and measured stable channel geometry should be one (Yadav et al. 2019). This study uses a DR of 0.8–1.2 (20% accuracy) to analyse the prediction model in multiple linear regression (MLR).

$$R^2 = \left[\frac{\sum\limits_{i=1}^{N}(O_i - \bar{O}_i)(P_i - \bar{P}_i)}{\sqrt{\sum\limits_{i=1}^{N}(O_i - \bar{O}_i)^2 \sum\limits_{i=1}^{N}(P_i - \bar{P}_i)^2}}\right]^2 \tag{1}$$

$$\text{NSE} = 1 - \left[\frac{\sum_{i=1}^{N} (O_i - P_i)^2}{\sum_{i=1}^{N} (O_i - \bar{O}_i)^2} \right] \tag{2}$$

$$\text{MAE} = \frac{1}{N} \sum_{i=1}^{N} |O_i - P_i| \tag{3}$$

$$\text{MSE} = \frac{1}{N} \sum_{i=1}^{N} (O_i - P_i)^2 \tag{4}$$

$$\text{DR} = \frac{P_i}{O_i} \tag{5}$$

RESULTS AND DISCUSSION

Stable channel geometry by using MLR analysis

The significance of each parameter in Table 4 was assessed to ascertain which parameter is influential to the stable channel geometry. The correlation analysis determines the significance of the parameter. The probability (p) value $< \alpha = 0.05$ indicates convincing evidence that the parameter is influencing the stable channel geometry. The results from the correlation analysis show that the stable channel geometry (B/y, B^*, y^*, S) were significant to the parameters Q^*, ψ, $V/\sqrt{gd_{50}(S_s - 1)}$, U^*/V, VS_o/ω_s, C_v, ϕ, D_{gr}, U^*/ω_s, $\omega_s d_{50}/v$, R/d_{50}, λ_s and V^2/gy. The selected best combination of characteristic parameters, together with the related equations from multiple linear analyses, were further assessed in the study of
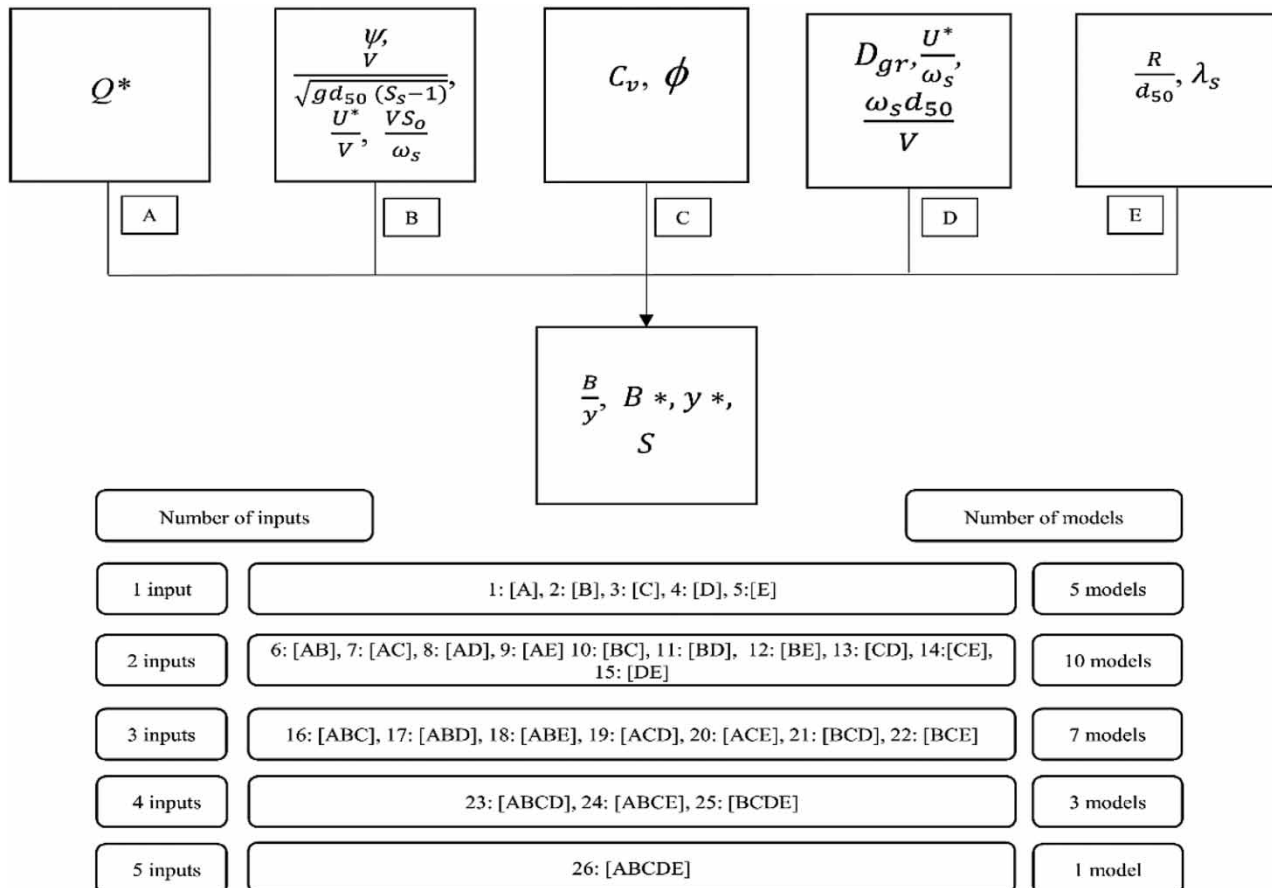
Figure 3 | Input combination for the stable geometry prediction.

variance (ANOVA) approach. Figure 3 explains the different input combinations for the determination of dimensionless width/depth, width, depth and the slope of a stable channel.

Width/depth (B/y) prediction

The B/y parameter was evaluated with a different combination of inputs, as shown in Figure 3. This study shows that B/y was significant to the combination of parameters Q^*, ψ, U^*/V, V/gd_{50} $(S_s - 1)$, VS_o/ω_s, D_{gr}, U^*/ω_s and R/d_{50}. In total, there were 37 combinations that were significant to the prediction of B/y. The best five combinations of the parameters are given in Table 5.

The R^2 value for model one is the highest among all the models (0.890) followed by model two (0.638), model three (0.598), model four (0.542) and model five (0.453). In contrast, MSE for model one yields the lowest MSE (45.549) followed by model two (157.900), model three (187.70), model four (208.298) and model five (253.270). As for the NSE, model one yields the highest value (0.889), followed by model two (0.614), model three (0.542), model four (0.492) and model five (0.382). A comparison between all models shows that model one yields the highest DR value which ranges between 0.8 and 1.2 (79.06%), and model five yields the lowest DR value (31.62%). The results of this study indicate that the B/y is best described by the combination parameters of Q^*, $V/\sqrt{gd_{50}\ (S_s - 1)}$ and R/d_{50}. The above findings conclude that model one is superior in comparison to the other models.

Width prediction by using dimensionless width (B*)

Results from the correlation analysis revealed that B^* was significant with the parameters Q^*, ϕ, ψ, U^*/V, VS_o/ω_s, V/gd_{50} $(S_s - 1)$, D_{gr}, U^*/ω_s, λ_s and R/d_{50}. There were 51 combination models altogether for the B^* prediction. Table 6 lists the best five combinations of the parameters that are significant to the B prediction.

Model one has the highest DR (93.16%), followed by model two (64.10%), model four (55.56%), model three (46.15%) and model five (37.61%). In terms of R^2, model one has the highest value (0.964), and model five has the lowest value (0.745). The trend was also the same for NSE, with model one showing the highest value (0.964), thereby indicating that the model predicts better compared to the other models. Moreover, model one tends to yield the lowest MAE (3,031.499); meanwhile, model five has the highest MAE among the models (10,167.036). Model one is considered superior compared to the other models because it has the highest R^2 and NSE and is able to give better DR that has 93.16% accuracy.

Mean depth prediction by using dimensionless depth (y*)

Significant parameters were combined to yield the best equation that can predict the average depth of the river. In the present study, it is observed that parameter Q^*, C_v, ϕ, ψ, VS_o/ω_s, V/gd_{50} $(S_s - 1)$, U^*/V, D_{gr}, λ_s and R/d_{50} were significant to the development of depth prediction. The analysis showed that 51 combination parameters were significant to the y^* prediction. Table 7 lists the best five combinations of parameters that are significant to the depth prediction.

Table 5 | Combination of model parameters for the B/y prediction

Model no.	Function	R^2	NSE	MSE	DR (%) (0.8–1.2)
1	$B/y = \mathbf{f}\left(Q^*, \dfrac{V}{\sqrt{gd_{50}\ (S_s - 1)}}, R/d_{50}\right)$	**0.890**	**0.889**	**45.549**	**79.06**
2	$B/y = \mathrm{f}\left(Q^*, \dfrac{VS_o}{\omega_s}, R/d_{50}\right)$	0.638	0.614	157.900	47.44
3	$B/y = \mathrm{f}(Q^*, \psi, R/d_{50})$	0.598	0.542	187.70	36.32
4	$B/y = \mathrm{f}\left(Q^*, \dfrac{U^*}{V}, R/d_{50}\right)$	0.542	0.492	208.298	33.76
5	$B/y = \mathrm{f}(Q^*, R/d_{50})$	0.453	0.382	253.270	31.62

The bold values highlight the best model for every stable channel geometry prediction.

Table 6 | Combination of model parameters for the width prediction

Model no.	Function	R^2	NSE	MSE	MAE	DR (0.8–1.2)
1	$B^* = f\left(Q^*, \dfrac{V}{\sqrt{gd_{50}\,(S_s - 1)}}, R/d_{50}\right)$	**0.964**	**0.964**	**40,203,592**	**3,031.499**	**93.16**
2	$B^* = f\left(Q^*, \dfrac{V}{\sqrt{gd_{50}\,(S_s - 1)}}\right)$	0.899	0.885	127,065,677	6,506.073	64.10
3	$B^* = f\left(Q^*, \dfrac{VS_o}{\omega_s}\right)$	0.790	0.784	238,754,794	8,740.868	46.15
4	$B^* = f\left(Q^*, \dfrac{VS_o}{\omega_s}, R/d_{50}\right)$	0.775	0.772	251,985,681	8,728.123	55.56
5	$B^* = f(Q^*, \psi, R/d_{50})$	0.745	0.743	284,390,597	10,167.036	37.61

The bold values highlight the best model for every stable channel geometry prediction.

Models one and two have the highest value of DR square (92.31%) followed by model three (91.88%), model four (91.45%) and model five (91.03%). Among all the models, Model two has the lowest in terms of MSE (58,451.679) and the highest in terms of R^2 (0.977) and NSE (0.977). Model two is selected to predict the depth instead of model one because model two gives a higher R^2 and NSE and the lowest MSE compared to the other models.

Slope (S) prediction

The prediction of the slope was calculated by combining the significant parameter, as discussed in Figure 3. In this study, parameters C_v, ϕ, ψ, VS_o/ω_s, D_{gr} and R/d_{50} were observed significant to the slope prediction. The study revealed that 57 models were significant to the slope prediction. The best five combinations for the slope prediction are listed in Table 8.

Model one has the highest R^2 (1) followed by model three (0.807), model two (0.795), model four (0.789) and model five (0.763). The same trend also applies to the NSE, but for MSE, the trend is in the reverse order. Model one has the lowest MSE, and model five has the highest MSE. Model one is found to be superior compared to the other models, as it has the highest DR ratio (100%) followed by model two (55.56%), model three (54.70%), model four (53.85%) and model five (50.43%).

The summary of the stable channel geometry prediction model in dimensionless form by using the MLR method is shown in Table 9.

Stable channel geometry by using GEP

The best model for every stable channel parameter was further determined by using GEP. The function for the stable hydraulic geometry was analysed based on the significant parameter, as shown in Table 9. The formulations of GEP for stable hydraulic geometry are shown in Table 10.

Table 7 | Combination of model parameters for the depth prediction

Model no.	Function	R^2	NSE	MSE	MAE	DR (0.8–1.2)
1	$Y^* = \left(\dfrac{V}{\sqrt{gd_{50}\,(S_s - 1)}}, R/d_{50}\right)$	0.976	0.976	61,362.717	113.724	92.31
2	$Y^* = \left(\dfrac{VS_o}{\omega_s}, R/d_{50}\right)$	**0.977**	**0.977**	**58,451.679**	**112.179**	**92.31**
3	$Y^* = (\psi, R/d_{50})$	0.974	0.974	64,305.962	117.158	91.88
4	$Y^* = \left(\dfrac{U^*}{V}, R/d_{50}\right)$	0.971	0.971	71,701.941	114.964	91.45
5	$Y^* = (Q^*, R/d_{50})$	0.972	0.972	70,137.137	121.286	91.03

The bold values highlight the best model for every stable channel geometry prediction.

Table 8 | Combination of model parameters for the slope prediction

Model no.	Function	R^2	NSE	MSE	DR (0.8–2.0)
1	$S = \mathrm{f}(\psi, R/d_{50})$	**1**	**0.9998**	$\mathbf{6.621 \times 10^{-12}}$	**100**
2	$S = f\left(C_v, , \dfrac{VS_o}{\omega_s}, D_{gr}, R/d_{50}\right)$	0.795	0.7854	7.868×10^{-8}	55.56
3	$S = \mathrm{f}(Q^*, \psi)$	0.807	0.802	7.083×10^{-8}	54.70
4	$S = f\left(C_v, \dfrac{VS_o}{\omega_s}, R/d_{50}\right)$	0.789	0.7764	8.009×10^{-8}	53.85
5	$S = f\left(\phi, \dfrac{VS_o}{\omega_s}, R/d_{50}\right)$	0.763	0.7527	8.886×10^{-8}	50.43

The bold values highlight the best model for every stable channel geometry prediction.

Table 9 | New equation for the stable geometry prediction by using the MLR method

Parameter	Equation	
B/y	$\dfrac{B}{y} = 0.537 \, Q*^{1.038} \left(\dfrac{V}{\sqrt{gd_{50}\,(S_s - 1)}}\right)^{-1.165} \left(\dfrac{R}{d_{50}}\right)^{-1.992}$	(6)
$B*$	$B* = 0.729 \, Q*^{1.018} \left(\dfrac{V}{\sqrt{gd_{50}\,(S_s - 1)}}\right)^{-1.08} \left(\dfrac{R}{d_{50}}\right)^{-0.992}$	(7)
$y*$	$y* = 1.432 \left(\dfrac{VS_o}{\omega_s}\right)^{0.029} \left(\dfrac{R}{d_{50}}\right)^{0.98}$	(8)
S	$S = 1.698 \, \psi^{-1.003} \left(\dfrac{R}{d_{50}}\right)^{-1.003}$	(9)

The performance of the training and testing of the GEP model is shown Table 11. The GEP model for all stable channel geometries has a high correlation for training and testing data. The same trend was also observed for the errors in terms of MSE and MAE.

The performance of the GEP model in comparison to the MLR model is shown in Table 12. Both models were analysed based on R^2, NSE, MSE and MAE. In all parameter predictions, GEP models outperformed MLR models, in which the GEP model yields better R^2 and NSE and produces the least errors in terms of MSE and MAE. It can be concluded that the GEP model is a far superior model compared to the traditional MLR method.

Evaluation of the existing equation and comparison with the newly developed equation

The performance of the currently developed equation by using MLR and GEP was compared to the previous equation (Figures 4–6), and the results are shown in Tables 13 and 14. The channel width, depth and slope of the stable channel are estimated by using the existing equation. As the equations were presented in dimensionless form, calculations of the width and the depth were done by multiplying the equation with d_{50}. For the B/y equation, the width is calculated by multiplying the equation by the depth of the channel. However, the equation will be divided by the width to obtain the depth of the channel.

In the prediction of channel width (B), the majority of the previous equations had moderate R^2 values but with low or negative values in terms of NSE. This shows that several of the equations were underpredicted, which explains the higher observed values compared to the predicted data. Only Pitlick & Cress (2002), Lee & Julien (2007) and Haron et al. (2019) have a positive value for NSE. Lee & Julien (2007) has the highest NSE of all, which is 0.61. Bonakdari et al. (2020) have the highest values of R^2 in EPR and GEP, namely, 0.685 and 0.655; however, these lack accuracy in the prediction, as the NSE value transpired to be negative. The NSE for both equations is -0.06 and -0.54, respectively. In terms of the error, Julien & Wargadalam (1995) have the highest MSE and MAE values, which are 1,335.68 and 24.76, respectively. Lee & Julien (2007) have

**Table 10** | New equation for the stable geometry prediction by using the GEP method

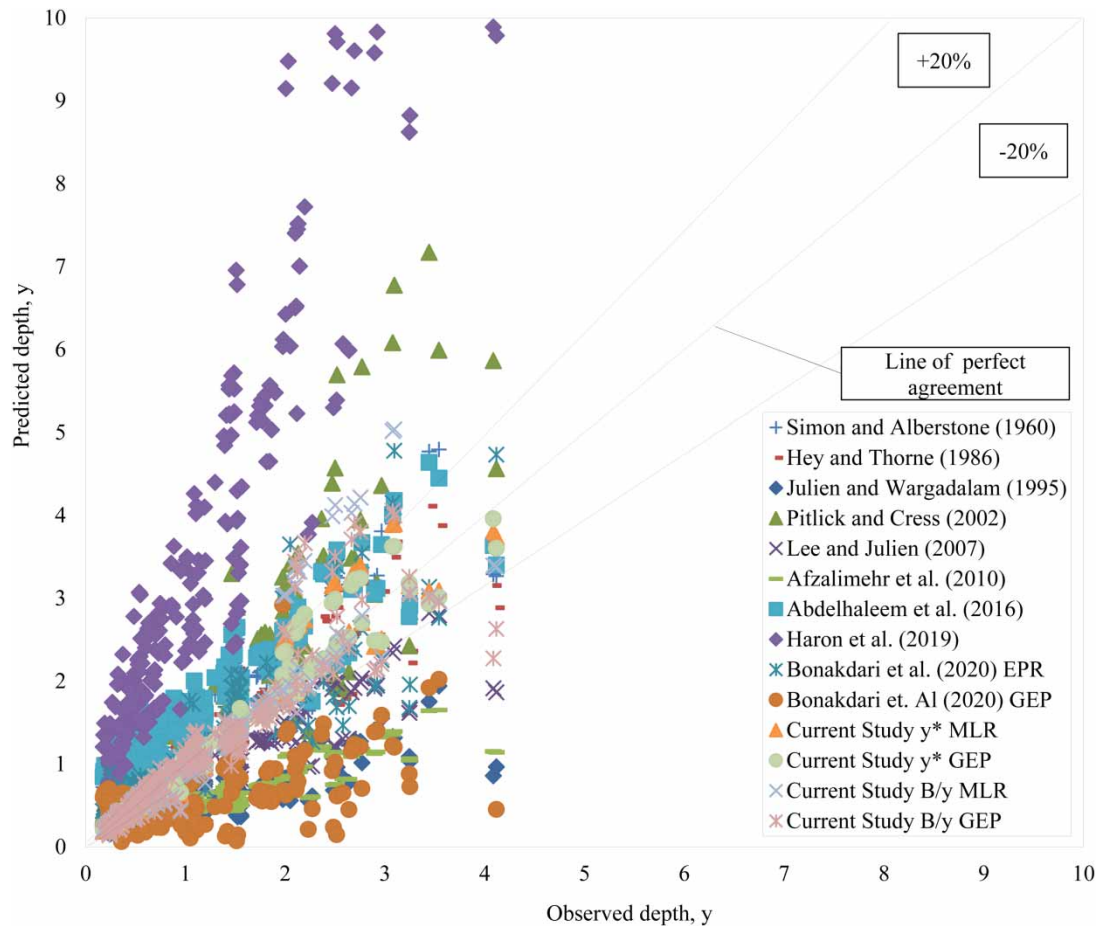| Parameter	Equation	
B/y	$$\frac{B}{y} = \left[\left(\frac{\dfrac{\dfrac{Q_*}{R}}{d_{50}}}{\dfrac{V}{\sqrt{gd_{50}\,(S_s - 1)}}}\right) \Big/ \left(\frac{R}{d_{50}} - 0.522034\right)\right] + \left[\frac{(9.536774 + 2.987488)}{\left(-0.020324 - \dfrac{V}{\sqrt{gd_{50}\,(S_s - 1)}}\right)}\right]$$	(10)
B_*	$$B_* = \left[\left(\left(Q_* + \frac{R}{d_{50}}\right) + \frac{R}{d_{50}} \times \frac{0.990571}{\dfrac{V}{\sqrt{gd_{50}\,(S_s - 1)}}}\right) \Big/ \left(\sqrt{\frac{R}{d_{50}}} - \left(-5.795624 - \frac{R}{d_{50}}\right)\right)\right]$$ $$+ \left[\left(\left(\frac{\dfrac{R}{d_{50}}}{Q_*} \times \frac{R}{d_{50}}\right) \times \left(-9.552795 \times \frac{V}{\sqrt{gd_{50}\,(S_s - 1)}}\right)\right) \times \left(\left(7.415771 \times \frac{R}{d_{50}}\right) + (-9.9949969.966462)\right)\right]$$ $$+ \left[\left(\left(\sqrt{\frac{R}{d_{50}}} - 6.941987\right) - (3.186157 - (-7.782227))\right) \times \left(\frac{\dfrac{V}{\sqrt{gd_{50}\,(S_s - 1)}} + \dfrac{R}{d_{50}}}{\dfrac{V}{\sqrt{gd_{50}\,(S_s - 1)}} + 4.669251}\right)\right]$$	(11)
y_*	$$y_* = \left[\left(\left(\frac{R}{d_{50}} + \frac{\dfrac{R}{d_{50}}}{-4.303009}\right) + 8.500763 \times (-6.995545) + 9.179809\right) + 7.762543\right]$$ $$+ \left[6.471924 \times \left(-3.832947 \times (-6.113281) \times \left(\frac{VS_o}{\omega_s} + 2.522461\right)\right) \times \left((-9.220377) \times \frac{VS_o}{\omega_s}\right)\right]$$ $$+ \left[\left(\left(-9.947205 + \frac{R}{d_{50}}\right) \times (-9.947205^2)\right) + \left(\left(7.781525 \times \frac{R}{d_{50}}\right) \times \left(\frac{R}{d_{50}} \times \frac{VS_o}{\omega_s}\right)\right)^{0.5}\right]$$	(12)
S	$$S = \left[2\left(\left(\frac{1}{\dfrac{-7.435791}{-7.43642}}\right) \Big/ \psi\right) \Big/ \frac{R}{d_{50}}\right] + \left[\left(\frac{\left(\left(\dfrac{-9.981672}{\psi}\right) \Big/ \left(\dfrac{R}{d_{50}} + \dfrac{R}{d_{50}}\right)\right)}{3.779541}\right) \Big/ 3.750305\right]$$	(13)

Table 11 | Evaluation of model performance for respective stable channel parameters in both training and testing stages in GEP

Parameter	Stage	R^2	MSE	MAE
B/y	Training	0.933	30.888	3.994
	Testing	0.806	49.228	4.26
$B*$	Training	0.972	27,800,000	3,171.487
	Testing	0.977	45,100,000	3,614,235
$y*$	Training	0.983	45,200	121.838
	Testing	0.980	41,400	125.52
S	Training	1	0	0
	Testing	1	0	0

Table 12 | Evaluation of the stable channel performance by using the MLR and GEP methods

Parameter	Model	R^2	NSE	MSE	MAE
B/y	MLR	0.890	0.889	45.549	4.697
	GEP	0.918	0.916	34.488	4.046
$B*$	MLR	0.964	0.964	40,203,592	3,031.499
	GEP	0.972	0.965	31,211,426	3,258.523
$y*$	MLR	0.977	0.977	5,8451.679	112.179
	GEP	0.982	0.982	45,470.525	126.021
S	MLR	1	0.999	6.622×10^{-12}	5.765×10^{-6}
	GEP	1	0.999	1.773×10^{-12}	1.092×10^{-6}
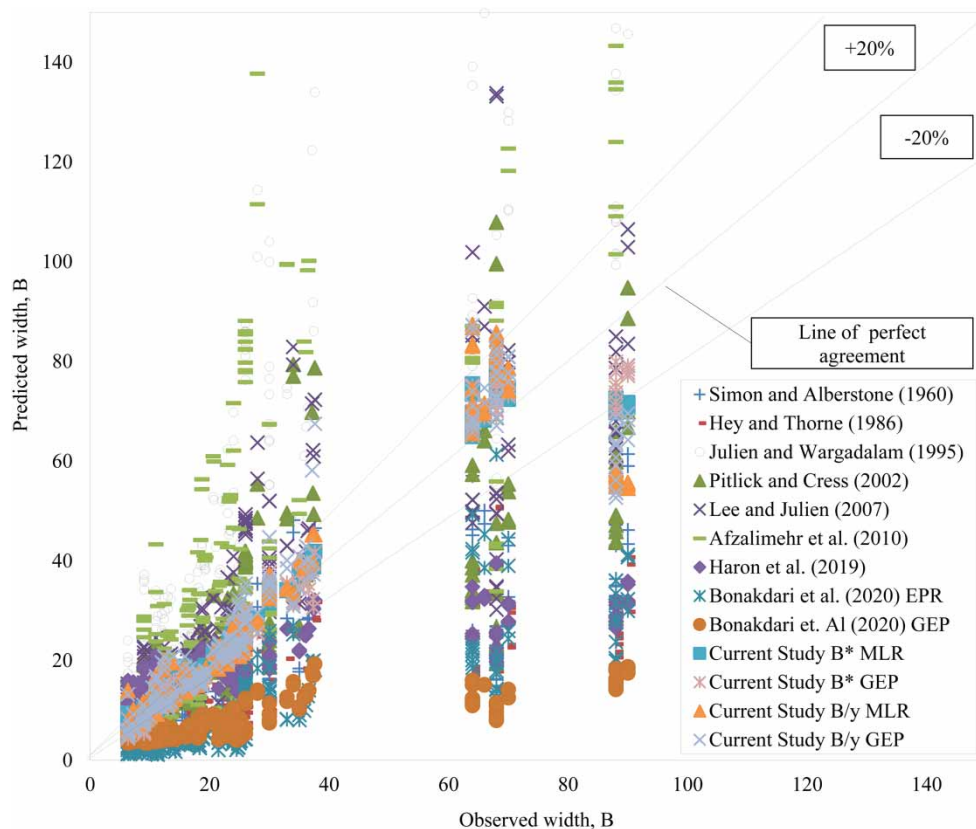
Figure 4 | Comparison of stable channel model performance by using the equation from previous researchers (width).
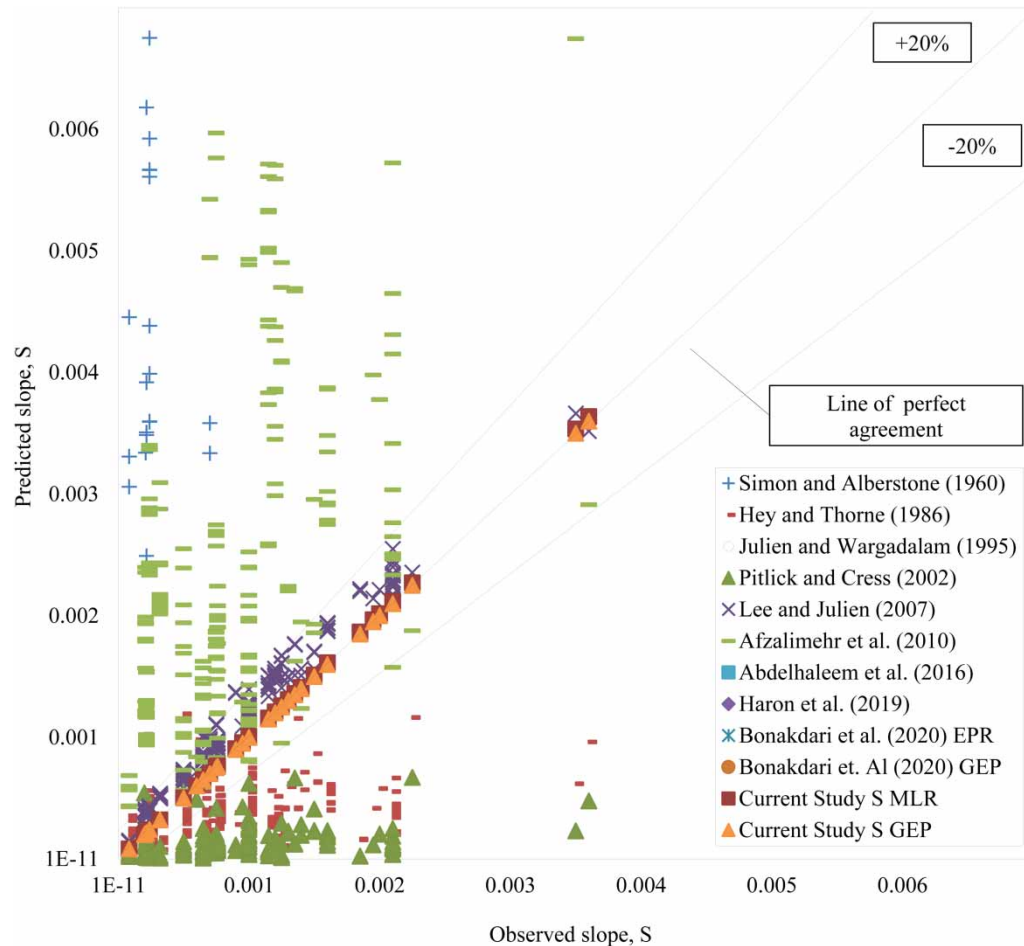
Figure 5 | Comparison of stable channel model performance by using the equation from previous researchers (depth).

the lowest MSE and MAE of all the equations (MSE = 206.52, MAE = 9.64). With the introduction of the new parameter, all newly developed equations were determined to give better stable channel width prediction. By using the MLR method, the current study MLR (B/y) and current study MLR (B) equations give higher R^2 and NSE values, and the revised equation, using GEP for both equations, returns improved R^2 and NSE values compared to the MLR method. The current study GEP (B) equation has the highest R^2 and NSE values, which are 0.965 and 0.965, followed by the current study MLR (B) equation ($R^2 = 0.953$, NSE = 0.953), the current study GEP (B/y) equation ($R^2 = 0.863$, NSE = 0.862) and the current study MLR (B/y) equation ($R^2 = 0.835$, NSE = 0.832). The trend for error indices is also the equivalent but in the reverse order. The current study GEP (B) equation has the lowest MSE and MAE values, which are 18.472 and 2.734, followed by the current study MLR (B) equation (MSE = 24.773, MAE = 2.674), the current study GEP (B/y) equation (MSE = 72.651, MAE = 4.811) and the current study MLR (B/y) equation (MSE = 88.308, MAE = 5.085).

In the prediction of flow mean depth y, many of the existing equations have high R^2 and NSE values, indicating that most of the equations are able to predict the depth of the river with low error (MSE and MAE). Hey & Thorne (1986), Lee & Julien (2007) and Bonakdari *et al.* (2020) EPR were particularly excellent in predicting the depth of the river with the DR (0.8–1.2) 39.32, 37.6 and 52.99%, respectively. Hey & Thorne (1986) have the lowest MSE (0.122) and MAE (0.282) among all the existing equations. Conversely, Simons & Alberstone (1960) have the highest MSE (40.49) and MAE (6.311). The newly developed equation is able to predict with better accuracy, coupled with less error. The current study GEP (y) equation has the highest R^2 and NSE values ($R^2 = 0.960$, NSE = 0.960) followed by the current study MLR (y) equation ($R^2 = 0.955$, NSE = 0.952), the current study GEP (B/y) equation ($R^2 = 0.839$, NSE = 0.819) and the current study MLR (B/y) equation ($R^2 = 0.839$, NSE = 0.783). The MSE and MAE of the newly developed equation were reduced to the ranges of 0.027–0.148 (MSE) and 0.095–0.195 (MAE).

Figure 6 | Comparison of stable channel model performance by using the equation from previous researchers (slope).

In the slope prediction, many existing equations are unable to predict the slope accurately, and many of the existing equations had low R^2 and NSE values. Julien & Wargadalam (1995) and Lee & Julien (2007) equations were found to be excellent in predicting the slope with an extremely high R^2 value (1, 0.982) and an high NSE value, which are 1.0 and 0.861, respectively. The MSE and MAE for both equations are also fairly low, being 3.131×10^{-11} and 4.985×10^{-8} (MSE), and 3.8467×10^{-6} and $2.054 \ 10^{-4}$ (MAE). In all the equations, the EPR and GEP equations of Bonakdari *et al.* (2020) were found to have the highest error. This may be due to the sensitivity of the equations used and is, therefore, not suitable for studying Malaysian rivers. The newly developed slope equation using GEP and MLR is able to predict with high R^2 and NSE values ($R^2 = 1$, NSE = 1). The MSE for both equations is fairly low, namely, 1.773×10^{-12} and 6.6217×10^{-12}, respectively, and MAE is 1.092×10^{-6} and 5.766×10^{-6}, respectively. Both Julien & Wargadalam (1995) and the current study equation (MLR and GEP) with fewer variables are determined to be suitable to predict the stable channel slope.

Validation of the developed equations

The presently developed equations were validated by using the data from Saleh *et al.* (2017, 2018), Chang *et al.* (2008), Sinnakaudan *et al.* (2006) and Ariffin (2004).

The results from Table 15 show that both MLR and GEP equations can predict the width of the river precisely. The R^2 and NSE values are high for all the validation data except for the current study GEP (B/y) equation and for the Ariffin (2004) data, in which the values for R^2 and NSE are 0.880 and 0.543, respectively. The predicted data are highly correlated but lack accuracy. This could be due to the fact that the GEP equation developed is sensitive to the characteristics of the current river data. The data from the Ariffin (2004) study are generally based on small river data. Conversely, the present study MLR (B/y)

Table 13 | Performance of different models for the stable channel prediction by previous researchers

Equations	B R^2	NSE	MSE	MAE	Y R^2	NSE	MSE	MAE	S R^2	NSE	MSE	MAE
Simons & Alberstone (1960)	0.595	−0.099	578.522	17.021	0.859	−72.748	40.492	6.311	0.199	−25.882	9.627×10^{-6}	0.00290
Hey & Thorne (1986)	0.606	−0.034	544.263	15.952	0.859	0.822	0.122	0.282	0.161	−5.544	5.261×10^{-7}	0.000530
Julien & Wargadalam (1995)	0.653	−1.537	1,335.683	24.759	0.758	0.026	0.667	0.598	1.000	1.000	3.131×10^{-11}	3.867×10^{-6}
Pitlick & Cress (2002)	0.548	0.532	246.420	10.074	0.790	0.224	0.531	0.427	0.120	−1.426	8.689×10^{-7}	0.000743
Lee & Julien (2007)	0.670	0.608	206.524	9.642	0.849	0.677	0.221	0.315	0.982	0.861	4.985×10^{-8}	0.000205
Afzalimehr et al. (2010)	0.524	−6.159	3,769.379	30.699	0.861	0.029	0.665	0.587	0.185	−13.155	5.070×10^{-6}	0.00166
Abdelhaleem et al. (2016)	–	–	–	–	0.865	0.441	0.383	0.576	0.166	−712,822	0.255	0.485
Haron et al. (2019)	0.620	0.207	417.707	11.893	0.834	−14.855	10.876	2.531	–	–	–	–
Bonakdari et al. (2020) EPR	0.685	−0.059	557.730	18.322	0.452	0.652	0.375	0.282	0.204	0.000	119.754	10.161
Bonakdari et al. (2020) GEP	0.655	−0.544	813.740	20.463	4.6×10^{-6}	−13.288	9.782	1.047	0.011	0.000	386,600,000	12,386.084
Current study MLR (B, y, S)	0.953	0.953	24.773	2.674	0.955	0.952	0.033	0.095	1.000	1.000	6.622×10^{-12}	5.765×10^{-6}
Current study GEP (B, y, S)	0.965	0.965	18.472	2.734	0.960	0.960	0.027	0.105	1.000	1.000	1.773×10^{-12}	1.0918×10^{-6}

Table 14 | Performance of the new B/y parameter for the stable channel prediction

Equations	B/y				B				y			
	R^2	NSE	MSE	MAE	R^2	NSE	MSE	MAE	R^2	NSE	MSE	MAE
Current study MLR (B/y)	0.890	0.889	45.549	4.697	0.835	0.832	88.308	5.085	0.839	0.783	0.148	0.193
Current study GEP (B/y)	0.918	0.916	34.488	4.046	0.863	0.862	72.651	4.811	0.839	0.819	0.124	0.195

equation is able to give far better results with better R^2 (0.954) and NSE (0.706) values. Overall, the new equation developed in this study is better in predicting the width compared to the existing equation.

Validation for the depth prediction in Table 16 shows that the developed MLR and GEP equations have an excellent degree of depth prediction accuracy based on the evidence of high R^2 and NSE values with low MSEs and MAEs. The current equation also outperformed the existing equations, as many of the existing equations yielded underpredicted values. However, the current study MLR (B/y) and current study GEP (B/y) equations yield low accuracy on the Saleh *et al.* (2017) data, whereby low R^2 and negative NSE values were observed. The model prediction is poorly correlated and inaccurate, as the predicted model performed worst. This could be due to the characteristics of the river that has a higher discharge compared to the current study data. This indicates that the equation is not suitable to apply to rivers with high discharge.

The slope validation prediction as shown in Table 17 revealed an equation from this study that is also able to predict the slope with high accuracy, particularly current study S (GEP), which yields better R^2 and NSE values and lower errors. This study also applies to the much-improved parameter that only consists of two parameters, namely, flow parameter and R/d_{50}.

As shown in Table 18, the new equation B/y also performed well in the validation data. The current study GEP (B/y) and and current study MLR equations have high R^2 and NSE values in all the validation data with low MSEs and MAEs. This indicates that parameter B/y is suitable to represent the geometry of the river. In the case of restriction either in the width or depth of the river, this equation is fundamental in helping decision-makers to determine the suitable channel dimension.

Limitation of the proposed model

The current study focuses on developing a new equation for stable channel geometry that is suitable for the median size of bed material between 0.29 and 3.0 mm. Different key geomorphological variables such as bank profile and vegetation types need to be considered in future studies to enhance researchers' understanding of the effect of changes to the stable channel geometry. Applications of different machine learning techniques with higher accuracy can be conducted to increase the accuracy of the model prediction. For the B/y model prediction, a different variable that resembles the hydraulic characteristic of the river should be further explored to increase the efficiency of the equation, especially in rivers with a high volume of discharge.

CONCLUSION

The current study set out to develop a new equation that can improve the stable channel geometry prediction accuracy. This study also aims to establish an equation in the dimensionless form of B/y to provide an alternative solution for the width and depth prediction. Existing equations predict stable channel geometry with low accuracy, as many model predictions use the same parameter. This research has enhanced our knowledge in predicting stable channel geometry by associating the sediment transport parameters to predict stable channel geometry. The newly proposed equations by using MLR and GEP give a better prediction for stable channel hydraulic geometry with a far better R^2, NSE and DR. Moreover, it was established that B/y is a good parameter that can be used to predict the geometry of the river. This result also suggests that the proposed MLR and GEP models are robust in predicting stable channel geometry, with lower MSEs and MAEs compared to the existing equations.

ACKNOWLEDGEMENTS

Table 15 | Validation results for the width model prediction

Equations	Ariffin (2004)				Sinnakaudan *et al.* (2006)				Chang *et al.* (2008)				Saleh *et al.* (2017)			
	R^2	NSE	MSE	MAE	R^2	NSE	MSE	MAE	R^2	NSE	MSE	MAE	R^2	NSE	MSE	MAE
Current study MLR (B/y)	0.954	0.706	1.725	0.775	0.908	0.880	1.807	0.922	0.898	0.760	2.411	1.236	0.915	0.914	1,266.136	11.707
Current study GEP (B/y)	0.880	0.543	2.682	0.630	0.920	0.892	1.623	0.534	0.900	0.833	1.676	1.039	0.800	0.789	3,104.135	20.043
Current study MLR (B)	0.984	0.927	0.427	0.367	0.975	0.972	0.430	0.428	0.975	0.943	0.570	0.599	0.837	0.833	2,451.964	19.813
Current study GEP (B)	0.963	0.873	0.748	0.753	0.963	0.912	1.334	0.921	0.993	0.684	3.176	1.758	0.916	0.914	1,262.937	13.856

Table 16 | Validation results for the depth model prediction

Equations	Ariffin (2004)				Sinnakaudan et al. (2006)				Chang et al. (2008)				Saleh et al. (2017)			
	R^2	NSE	MSE	MAE	R^2	NSE	MSE	MAE	R^2	NSE	MSE	MAE	R^2	NSE	MSE	MAE
Current study MLR (B/y)	0.980	0.948	0.006	0.028	0.983	0.960	0.005	0.031	0.931	0.636	0.008	0.079	0.352	−0.257	2.101	0.502
Current study GEP (B/y)	0.906	0.901	0.012	0.033	0.944	0.943	0.007	0.026	0.925	0.882	0.002	0.039	0.230	−0.049	1.753	0.455
Current study MLR (y)	0.998	0.990	0.001	0.031	0.996	0.990	0.001	0.027	0.981	0.825	0.003	0.055	0.914	0.916	0.140	0.141
Current study GEP (y)	0.989	0.854	0.017	0.045	0.956	0.918	0.010	0.045	0.995	0.707	0.006	0.076	0.924	0.918	0.136	0.167

Table 17 | Validation results for the width slope prediction

Equations	Ariffin (2004)				Sinnakaudan et al. (2006)				Chang et al. (2008)				Saleh et al. (2017)			
	R^2	NSE	MSE	MAE	R^2	NSE	MSE	MAE	R^2	NSE	MSE	MAE	R^2	NSE	MSE	MAE
Current study MLR (S)	1.000	0.999	6.951×10^{-9}	7.041×10^{-5}	1.000	1.000	3.436×10^{-9}	0.0000399	1.000	0.893	4.169×10^{-11}	6.454×10^{-6}	1.000	1.000	9.262×10^{-10}	2.138×10^{-5}
Current study GEP (S)	1.000	1.000	6.697×10^{-11}	7.306×10^{-6}	1.000	1.000	3.430×10^{-11}	0.0000045	1.000	1.000	1.568×10^{-12}	4.47×10^{-6}	1.000	1.000	3.430×10^{-11}	4.47×10^{-6}

Table 18 | Validation results for the *B/y* model prediction

Equations	Ariffin (2004)				Sinnakaudan *et al.* (2006)				Chang *et al.* (2008)				Saleh *et al.* (2017)			
	R^2	NSE	MSE	MAE	R^2	NSE	MSE	MAE	R^2	NSE	MSE	MAE	R^2	NSE	MSE	MAE
Current study MLR (*B/y*)	0.987	0.963	5.321	1.717	0.993	0.970	7.792	1.929	0.938	0.806	11.770	2.684	0.864	0.858	1,883.431	13.716
Current study GEP (*B/y*)	0.991	0.990	1.499	0.802	0.996	0.996	1.158	0.741	0.932	0.886	6.910	2.139	0.866	0.863	1,820.116	11.504

DATA AVAILABILITY STATEMENT

Data cannot be made publicly available; readers should contact the corresponding author for details.

REFERENCES

Abdelhaleem, F. S., Amin, A. M. & Ibraheem, M. M. 2016 Updated regime equations for alluvial Egyptian canals. *Alexandria Engineering Journal* **55** (1), 505–512. doi:10.1016/j.aej.2015.12.011.

Ab. Ghani, A., Zakaria, N. A., Abdullah, R., Chang, C. K., Sinnakaudan, S. K. & Mohd Sidek, L. 2003 *Guidelines for Field Data Collection and Analysis of River Sediment*. Department of Drainage and Irrigation Malaysia, Kuala Lumpur, Malaysia.

Abou-Seida, M. M. & Saleh, M. 1987 Design of stable alluvial channels. *Journal of Hydraulic Research* **25** (4), 433–446. doi:10.1080/00221688709499261.

Afzalimehr, H., Abdolhosseini, M. & Singh, V. P. 2010 Hydraulic geometry relations for stable channel design. *Journal of Hydrologic Engineering* **15** (10), 859–864. doi:10.1061/(ASCE)HE.1943-5584.0000260.

Ariffin, J. 2004 *Development of Sediment Transport Models for Rivers in Malaysia Using Regression Analysis and Artificial Neural Network*. PhD Thesis. Universiti Sains Malaysia, Penang, Malaysia.

Asheghi, R., Hosseini, S. A., Saneie, M. & Shahri, A. A. 2020 Updating the neural network sediment load models using different sensitivity analysis methods: a regional application. *Journal of Hydroinformatics* **22** (3), 562–577. doi:10.2166/hydro.2020.098.

Bennett, N. D., Croke, B. F. W., Guariso, G., Guillaume, J. H. A., Hamilton, S. H., Jakeman, A. J. & Andreassian, V. 2013 Characterising performance of environmental models. *Environmental Modelling and Software* **40**, 1–20. doi:10.1016/j.envsoft.2012.09.011.

Blench, T. 1957 *Regime Behavior of Canals and Rivers*. Butterworths, London.

Bonakdari, H., Gholami, A., Sattar, A. M. A. & Gharabaghi, B. 2020 Development of robust evolutionary polynomial regression network in the estimation of stable alluvial channel dimensions. *Geomorphology* **350**, 106895. doi:10.1016/j.geomorph.2019.106895.

Chang, H. H. 1988 *Fluvial Process in River Engineering*. Wiley-Interscience, USA.

Chang, C. K., Ab Ghani, A., Abdullah, R. & Zakaria, N. A. 2008 Sediment transport modeling for Kulim River: a case study. *Journal of Hydro-Environment Research* **2** (1), 47–59. doi:10.1016/j.jher.2008.04.002.

Copeland, R. R. 1994 *Application of Channel Stability Methods Case Studies*. Technical Report No. HL-94-11. Waterways Experiment Station, Vicksburg, Mississippi.

Danandeh Mehr, A. & Safari, M. J. S. 2020 Application of soft computing techniques for particle Froude number estimation in sewer pipes. *Journal of Pipeline Systems Engineering and Practice* **11** (2), 1–8. doi:10.1061/(ASCE)PS.1949-1204.0000449.

Deshpande, V. & Kumar, B. 2012 Review and assessment of the theories of stable alluvial channel design. *Water Resources* **39** (4), 481–487. doi:10.1134/S0097807812040033.

DID 2009 *River Sand Mining Management Guideline*. Department of Drainage and Irrigation Malaysia, Kuala Lumpur, Malaysia.

Ebtehaj, I. & Bonakdari, H. 2016 Bed load sediment transport estimation in a clean pipe using multilayer perceptron with different training algorithms. *KSCE Journal of Civil Engineering* **20** (2), 581–589. doi:10.1007/s12205-015-0630-7.

Ebtehaj, I. & Bonakdari, H. 2017 No-deposition sediment transport in sewers using of gene expression programming. *Soft Computing in Civil Engineering* **1** (1), 29–53.

Ebtehaj, I., Bonakdari, H., Safari, M. J. S., Gharabaghi, B., Zaji, A. H., Riahi Madavar, H., Sheikh Khozani, Z., Es-haghi, M. S., Shishegaran, A. & Danandeh Mehr, A. 2019 Combination of sensitivity and uncertainty analyses for sediment transport modeling in sewer pipes. *International Journal of Sediment Research* **35**, 157–170. doi:10.1016/j.ijsrc.2019.08.005.

Ferreira, C. 2001a Gene expresion programming: a new adaptive algorithm for solving problem. *Complex Systems* **13** (2), 87–129.

Ferreira, C. 2001b Gene expression programming in problem solving. In: *6th Online World Conference on Soft Computing in Industrial Applications*. Springer, Berlin, Germany.

Garcia, M. H. 2008 *Sedimentation Engineering: Processes, Measurements, Modeling, and Practice*. Reston, Virginia. https://doi.org/10.1061/9780784408230.

Gholami, A., Bonakdari, H., Ebtehaj, I., Shaghaghi, S. & Khoshbin, F. 2017 Developing an expert group method of data handling system for predicting the geometry of a stable channel with a gravel bed. *Earth Surface Processes and Landforms* **42** (10), 1460–1471. doi:10.1002/esp.4104.

Gholami, A., Bonakdari, H., Zeynoddin, M., Ebtehaj, I., Gharabaghi, B. & Khodashenas, S. R. 2018 Reliable method of determining stable threshold channel shape using experimental and gene expression programming techniques. *Neural Computing and Applications* **31** (10), 5799–5817. doi:10.1007/s00521-018-3411-7.

Gholami, A., Bonakdari, H., Ebtehaj, I., Talesh, S. H. A., Khodashenas, S. R. & Jamali, A. 2019a Analyzing bank profile shape of alluvial stable channels using robust optimization and evolutionary ANFIS methods. *Applied Water Science* **9** (3). doi:10.1007/s13201-019-0928-6.

Gholami, A., Bonakdari, H., Samui, P., Mohammadian, M. & Gharabaghi, B. 2019b Predicting stable alluvial channel profiles using emotional artificial neural networks. *Applied Soft Computing Journal* **78**, 420–437. doi:10.1016/j.asoc.2019.03.003.

Giustolisi, O. & Savic, D. 2009 Advances in data-driven analyses and modelling using EPR-MOGA. *Journal of Hydroinformatics* **11** (3–4), 225–236. doi:10.2166/hydro.2009.017.

Hadadin, N. 2017 Variation in hydraulic geometry for stable versus incised streams in the Yazoo River basin – USA. *International Journal of Sediment Research* **32** (1), 121–126. doi:10.1016/j.ijsrc.2016.03.003.

Haron, N. A., Yusuf, B., Sulaiman, M. S., Ab Razak, M. S. & Abu Bakar, S. N. 2019 Assessing river stability and hydraulic geometry of fluvial river in Malaysia. *International Journal of Integrated Engineering* **11** (6), 214–223. doi:10.30880/ijie.2019.11.06.023.

Harun, M. A., Ab. Ghani, A., Mohammadpour, R. & Chan, N. W. 2020 Stable channel analysis with sediment transport for rivers in Malaysia: a case study of the Muda, Kurau, and Langat rivers. *International Journal of Sediment Research* **35**, 455–466. doi:10.1016/j.ijsrc.2020.03.008.

Hey, R. D. & Thorne, C. R. 1986 Stable channels with mobile gravel beds. *Journal of Hydraulic Engineering* **112** (8), 671–689. doi:10.1061/(ASCE)0733-9429(1986)112:8(671).

Jang, E. K., Ji, U., Kim, K. H. & Yeo, W. K. 2016 Stable channel design with different sediment transport equations and geomorphologic constraints in Cheongmi stream. *KSCE Journal of Civil Engineering* **20** (5), 2041–2049. doi:10.1007/s12205-015-0126-5.

Julien, P. Y. & Wargadalam, J. 1995 Alluvial channel geometry: theory and applications. *Journal of Hydraulic Engineering* **121** (4), 312–325.

Julien, P. Y., Ab. Ghani, A., Zakaria, N. A., Abdullah, R. & Chang, C. K. 2010 Case study: flood mitigation of the Muda River, Malaysia. *Journal of Hydraulic Engineering* **136** (4), 251–261. doi:10.1061/(ASCE)HY.1943-7900.0000163.

Kaless, G., Mao, L. & Lenzi, M. A. 2014 Regime theories in gravel-bed rivers: models, controlling variables, and applications in disturbed Italian rivers. *Hydrological Processes* **28** (4), 2348–2360. doi:10.1002/hyp.9775.

Kargar, K., Safari, M. J. S., Mohammadi, M. & Samadianfard, S. 2019 Sediment transport modeling in open channels using neuro-fuzzy and gene expression programming techniques. *Water Science and Technology* **79** (12), 2318–2327. doi:10.2166/wst.2019.229.

Kennedy, R. G. 1895 The prevention of silting in irrigation canals. *Minutes of the Proceedings of the Institution of Civil Engineers* **119** (1895), 281–290. doi:10.1680/imotp.1895.19850.

Khosravi, M. & Javan, M. 2019 Prediction of side thermal buoyant discharge in the cross flow using multi-objective evolutionary polynomial regression (EPR-MOGA). *Journal of Hydroinformatics* **21** (6), 980–998. doi:10.2166/hydro.2019.010.

Koza, J. R. 1994 Genetic programming as a means for programming computers by natural selection. *Statistics and Computing* **4** (2), 87–112. doi:10.1007/BF00175355.

Lacey, G. 1930 Stable channels in alluvium. *Minutes of the Proceedings of the Institution of Civil Engineers* **229** (1930), 259–292. doi:10.1680/imotp.1930.15592.

Lee, J. & Julien, P. Y. 2007 Downstream hydraulic geometry of alluvial channels. *Journal of Hydraulic Engineering* **132** (12), 1347–1352.

Leopold, L. & Maddock, T. 1953 *The Hydraulic Geometry of Streams Channel and Some Physiographic Implications*. U.S. Geological Survey Professional Paper 252, 55.

Lindley, E. S. 1919 Regime channels. *Punjab Engineering Congress* **7**, 63.

Montes, C., Berardi, L., Kapelan, Z. & Saldarriaga, J. 2020 Predicting bedload sediment transport of non-cohesive material in sewer pipes using evolutionary polynomial regression–multi-objective genetic algorithm strategy. *Urban Water Journal* **17** (2), 154–162. doi:10.1080/1573062X.2020.1748210.

Muhammad, M. M., Yusof, K. W., Ul Mustafa, M. R., Zakaria, N. A. & Ghani, A. A. 2018 Artificial neural network applications for predicting drag coefficient in flexible vegetated channels. *Journal of Telecommunication, Electronic and Computer Engineering* **10** (1–12), 99–102.

Najafzadeh, M. & Oliveto, G. 2020 Riprap incipient motion for overtopping flows with machine learning models. *Journal of Hydroinformatics* **22** (4), 749–767. doi:10.2166/hydro.2020.129.

Parker, G. 1978 Self-formed straight rivers with equilibrium banks and mobile bed. Part 2. The gravel river. *Journal of Fluid Mechanics* **89**, 127–146.

Parker, G. 1979 Hydraulic geometry of active gravel rivers. *Journal of the Hydraulics Division* **105** (HY9), 1185–1201.

Pitlick, J. & Cress, R. 2002 Downstream changes in the channel geometry of a large gravel bed river. *Water Resources Research* **38** (10), 34-1–34-11. doi:10.1029/2001wr000898.

Roushangar, K. & Ghasempour, R. 2019 Evaluation of the impact of channel geometry and rough elements arrangement in hydraulic jump energy dissipation via SVM. *Journal of Hydroinformatics* **21**, 92–103. doi:10.2166/hydro.2018.028.

Roushangar, K. & Shahnazi, S. 2020 Prediction of sediment transport rates in gravel-bed rivers using Gaussian process regression. *Journal of Hydroinformatics* **22** (2), 249–262. doi:10.2166/hydro.2019.077.

Saleh, A., Abustan, I., Mohd Remy Rozainy, M. A. Z. & Sabtu, N. 2017 Assessment of total bed material equations on selected Malaysia rivers. *AIP Conference Proceedings* **1892**, 070002. doi:10.1063/1.5005720.

Saleh, A., Abustan, I., Mohd Remy Rozainy, Z. & Sabtu, N. 2018 Sediment transport and characteristics in Perak River and Kurau River. *International Journal of Engineering & Technology* **7**, 849–852. doi:10.14419/ijet.v7i2.29.14270.

Shaghaghi, S., Bonakdari, H., Gholami, A., Kisi, O., Binns, A. & Gharabaghi, B. 2018 Predicting the geometry of regime rivers using M5 model tree, multivariate adaptive regression splines and least square support vector regression methods. *International Journal of River Basin Management* **17** (3), 333–352. doi:10.1080/15715124.2018.1546731.

Sharafati, A., Tafarojnoruz, A., Motta, D. & Yaseen, Z. M. 2020 Application of nature-inspired optimization algorithms to ANFIS model to predict wave-induced scour depth around pipelines. *Journal of Hydroinformatics* **22** (6), 1425–1451. doi:10.2166/HYDRO.2020.184.

Sim, L. M., Chan, N. W. & Ao, M. 2015 Stakeholders' participation in sustainable water resource management: a case study of Muda River basin. In: *6th International Academic Consortium for Sustainable Cities (IACSC) Symposium*.

Simons, D. B. & Albertson, M. L. 1960 Uniform water conveyance channels in alluvial materials. *Journal of Hydraulic Diversion* **128**, 165–167.

Singh, V. P. 2003 On the theories of hydraulic geometry. *International Journal of Sediment Research* **18** (3), 196–218.

Sinnakaudan, S. K., Ghani, A. A., Ahmad, M. S. S. & Zakaria, N. A. 2006 Multiple linear regression model for total bed material load prediction. *Journal of Hydraulic Engineering* **132** (5), 521–528. https://doi.org/10.1061/(ASCE)0733-9429(2006)132:5(521).

Yadav, S. M., Yadav, V. K. & Gilitwala, A. 2019 Evaluation of bed load equations using field measured bed load and bed material load. *ISH Journal of Hydraulic Engineering*, 1–11. doi:10.1080/09715010.2019.1594417.

Yahaya, A. S. 2019 Application of statistical techniques in environmental modelling. *AIP Conference Proceedings* **2129**, 020074. doi:10.1063/1.5118082.

Yalin, M. S. & Ferreira Da Silva, A. M. 2000 Computation of regime channel characteristics on thermodynamic basis. *Journal of Hydraulic Research* **38** (1), 57–63. doi:10.1080/00221680009498359.